Generalized Scattering Matrix Synthesis for Hybrid Systems with Multiple Scatterers and Antennas Using Independent Structure Simulations

Chenbo Shi, Shichen Liang, Jin Pan, Xin Gu and Le Zuo

Abstract—This paper presents a unified formulation for calculating the generalized scattering matrix (GS-matrix) of hybrid systems involving multiple scatterers and antennas. The GS-matrix of the entire system is synthesized through the scattering matrices and GS-matrices of each independent component, using the addition theorem of vector spherical wavefunctions and fully matrix-based operations. Since our formulation is applicable to general antenna-scatterer hybrid systems, previous formulas for multiple scattering and antenna arrays become special cases of our approach. This also establishes our formulation as a universal domain decomposition method for analyzing the electromagnetic performance of hybrid systems. We provide numerous numerical examples to comprehensively demonstrate the capabilities and compatibility of the proposed formulation, including its potential application in studying the effects of structural rotation.

Index Terms—Generalized scattering matrix, scattering matrix, domain decomposition, multiple scattering, antenna array.

I. INTRODUCTION

THE scattering matrix (S-matrix) of a scatterer is a key tool in describing how it modifies (scatters) the incoming electromagnetic fields. It is typically defined using the expansion of vector spherical wavefunctions (VSWFs) [1]. By leveraging the addition theorem of VSWFs [2], [3], the mutual coupling between different structures can be analytically modeled, allowing the decomposition of complex problems into smaller, more manageable single-structure analyses. This approach significantly accelerates computation without sacrificing accuracy and is widely used in multiple scattering problems [4]–[7] and the fast decomposition of characteristic modes [8].

Building on this, researchers have introduced the generalized scattering matrix (GS-matrix) [9], which takes into account the port excitations of antennas. This formulation is applicable to various scenarios, including spherical near-field measurements [10], minimum-scattering antenna design [11], [12], and high-precision prediction of antenna arrays [13].

However, a key limitation of these methods is that they primarily address pure systems of either scatterers or antennas. Few studies have extended these techniques to efficiently

Manuscript received Nov. 19, 2024. (Corresponding author: Jin Pan.) Chenbo Shi, Shichen Liang, Jin Pan and Xin Gu are with the School of Electronic Science and Engineering, University of Electronic Science and Technology of China, Chengdu 611731 China (e-mail: chenbo_shi@163.com; xin_gu04@163.com; lscstu001@163.com; panjin@uestc.edu.cn).

Le Zuo is with The 29th Research Institute of China Electronics Technology Group Corporation (e-mail: zorro1204@163.com)

analyze hybrid systems involving both antennas and scatterers, even though such hybrid systems are more commonly encountered in practice. For instance, even a single antenna may still interact with the Earth's scattering background.

Recently, an extension method [14] has been proposed to analyze hybrid systems comprising one antenna and one scatterer, yielding promising results. However, this framework is unsuitable for effective domain decomposition in systems with multiple antennas and scatterers, as it requires treating all antennas as a single multi-port antenna and all scatterers as one large scatterer. Additionally, the addition theorem of VSWFs imposes a constraint that the minimum circumscribing spheres of different structures must not overlap, which further limits the applicability of [14]. For instance, in a scenario where a scatterer is positioned between two antennas, treating the antennas as a single multi-port structure results in a circumscribing sphere intersecting with the scatterer, making the method in [14] ineffective.

The goal of this paper is to extend the approach in [14] to address general hybrid systems involving multiple antennas and scatterers, overcoming the limitations on the number of structures. We establish an algebraic relationship between the entire system's GS-matrix and S/GS-matrices of its individual components, using a fully matrix-based operation derived from the addition theorem of VSWFs. This relationship is both concise and physically insightful.

As further discussed in this paper, our results provide a unified framework that serves as a universal approach to domain decomposition in multi-structured systems. Specifically, the formulas for pure antenna systems and pure scatterer systems emerge as special cases of the general formulation presented here. We demonstrate the versatility of the method with several examples, including pure scatterer systems, pure antenna systems, and scatterer-antenna hybrid systems. These numerical examples not only validate the proposed formulas but also showcase a potential application of GS-matrix in studying the rotational effects of structures.

II. A REVIEW OF GENERALIZED SCATTERING MATRIX

Figure 1 illustrates the typical scenario inscribed by the GS-matrix, where the in- and out-states include the incoming and outgoing VSWFs outside the circumscribing sphere (with expansion vectors **a** and **b**, respectively), as well as the incident and outgoing eigenmodes of the waveguide transmission line (with expansion vectors **v** and **w**, respectively). Following

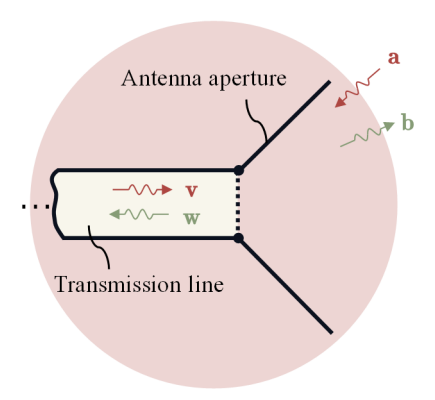


Fig. 1. A typical system where the in- and out-states involve both spatial transmission waves and guided waves in the transmission line.

the notation conventions in [15], the GS-matrix into matrixpartition form is written as

$$\tilde{\mathbf{S}} = \begin{bmatrix} \mathbf{\Gamma} & \mathbf{R} \\ \mathbf{T} & \mathbf{S} \end{bmatrix} \tag{1}$$

and

$$\begin{bmatrix} \mathbf{w} \\ \mathbf{b} \end{bmatrix} = \begin{bmatrix} \mathbf{\Gamma} & \mathbf{R} \\ \mathbf{T} & \mathbf{S} \end{bmatrix} \begin{bmatrix} \mathbf{v} \\ \mathbf{a} \end{bmatrix}. \tag{2}$$

For a reciprocal system, $\tilde{\mathbf{S}} = \tilde{\mathbf{S}}^t$, and for a lossless system, $\tilde{\mathbf{S}}^{\dagger}\tilde{\mathbf{S}} = \mathbf{1}$, where the superscripts t and † represent transpose and conjugate transpose, respectively.

More commonly used in practical problems is the following variant that strips away the natural transformation between inand out- states that is irrelevant of the structure properties:

$$\begin{bmatrix} \mathbf{w} \\ \mathbf{f} \end{bmatrix} = \begin{bmatrix} \mathbf{\Gamma} & \mathbf{R} \\ \mathbf{T} & \mathbf{S} - \mathbf{1} \end{bmatrix} \begin{bmatrix} \mathbf{v} \\ \mathbf{a} \end{bmatrix} \tag{3}$$

where a represents the expansion vector of the incident waves now, and $\mathbf{f} = \mathbf{b} - \mathbf{a}$ represents the expansion vector of the scattered waves. This formulation facilitates modeling mutual coupling between structures and serves as the fundamental equation in this paper.

There are two degenerate forms of (3). If the structure is a pure scatterer with no waveports, only the bottom-right block S-1 remains, *i.e.*,

$$\mathbf{f} = (\mathbf{S} - 1)\mathbf{a}.\tag{4}$$

If the structure is a waveguide system without radiation, only the top-left block Γ remains, *i.e.*, $\mathbf{w} = \Gamma \mathbf{v}$. Note that in scattering theory and microwave circuit theory, both \mathbf{S} and Γ are referred to as "S-matrix". However, in this paper, we distinguish Γ as the "S-parameter matrix".

The GS-matrix can be computed using methods such as the finite element method [13] or the method of moments (MoM) [15]. In particular, for the MoM-based approach, $\tilde{\mathbf{S}}$ can be succinctly expressed as

$$\tilde{\mathbf{S}} = -2\tilde{\mathbf{P}}\mathbf{Z}^{-1}\tilde{\mathbf{P}}^t + \tilde{\mathbf{I}} \tag{5}$$

where \mathbf{Z} is the impedance matrix, $\tilde{\mathbf{P}}$ is a projection matrix that links electromagnetic current to its corresponding radiation fields, and $\tilde{\mathbf{1}}$ is a special identity matrix. While (5) is also applicable to hybrid systems comprising multiple antennas

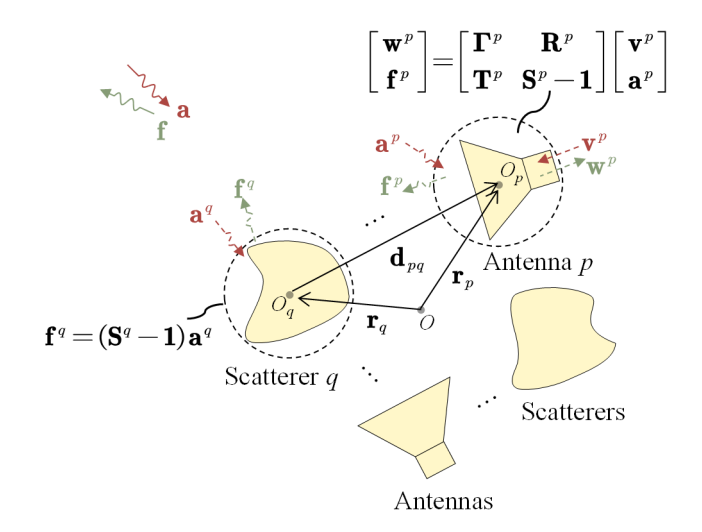


Fig. 2. Hybrid system of multiple antennas and scatterers.

and scatterers, it requires solving the inverse of the entire system's impedance matrix, which can be computationally expensive. Therefore, we only uses (5) to obtain GS-matrices of individual components and focuses on synthesizing the GS-matrix of the entire system with these individual results.

III. SYNTHESIS OF THE GENERALIZED SCATTERING MATRIX FOR ANTENNA-SCATTERER HYBRID SYSTEM

Consider a system consisting of M antennas and N scatterers, forming a total of M+N structures labeled as $p=1,2,\cdots,M,M+1,\cdots,M+N$, as illustrated in Fig. 2. We define the set $A=1,2,\cdots,M$ to label the antennas and the set $S=M+1,M+2,\cdots,M+N$ to label the scatterers, $viz., p\in A\cup S$. Using the independent GS- or S-matrix of the p-th structure, we can establish the relationships between the incident waves and scattered waves of each structure as follows 1 :

$$\begin{cases} \mathbf{\Gamma}^{p} \mathbf{v}^{p} + \mathbf{R}^{p} \mathbf{a}^{p} = \mathbf{w}^{p} \\ \mathbf{T}^{p} \mathbf{v}^{p} + (\mathbf{S}^{p} - 1) \mathbf{a}^{p} = \mathbf{f}^{p} \end{cases}, p \in A$$
 (6)

and

$$(\mathbf{S}^p - \mathbf{1})\mathbf{a}^p = \mathbf{f}^p, \ p \in S. \tag{7}$$

The incident vector \mathbf{a}^p generally includes the direct incident vector \mathbf{a}^p_d (e.g., plane wave incidence) and the secondary incidence from the q-th structure's scattered wave \mathbf{f}^q ($q \neq p$). Thus, we have

$$\mathbf{a}^p = \mathbf{a}_d^p + \sum_{q \neq p} \mathcal{G}_{pq} \mathbf{f}^q \tag{8}$$

where $\mathcal{G}_{pq} = \mathcal{G}(k\mathbf{d}_{pq})$ is a translation matrix that maps the scattered wave from the q-th local coordinate system to the incident wave at the p-th local coordinate system (see Appendix A for details on these matrices), and k represents

¹In this paper, structure's independent GS- or S-matrix is calculated in the local coordinate system with its geometric center as the origin. Note that the axes directions of different local coordinate systems should align with those of the global coordinate system to ensure they overlap upon translation.

free space wavenumber. Note that in (8), q iterates over the entire set $A \cup S$, and the equation holds for any $p \in A \cup S$. Substituting (8) into (6) and (7) yields

$$\begin{cases}
\mathbf{\Gamma}^{p} \mathbf{v}^{p} + \mathbf{R}^{p} \mathbf{a}_{d}^{p} + \mathbf{R}^{p} \sum_{q \neq p} \mathcal{G}_{pq} \mathbf{f}^{q} = \mathbf{w}^{p} \\
\mathbf{T}^{p} \mathbf{v}^{p} + (\mathbf{S}^{p} - 1) \mathbf{a}_{d}^{p} + (\mathbf{S}^{p} - 1) \sum_{q \neq p} \mathcal{G}_{pq} \mathbf{f}^{q} = \mathbf{f}^{p}
\end{cases} (9)$$

for $p \in A$, and

$$(\mathbf{S}^p - \mathbf{1}) \mathbf{a}_d^p + (\mathbf{S}^p - \mathbf{1}) \sum_{q \neq p} \mathbf{\mathcal{G}}_{pq} \mathbf{f}^q = \mathbf{f}^p$$
 (10)

for $p \in S$. Iterating the index p across the entire set $A \cup S$ yields a system of well-posed equations. However, solving these equations directly can be cumbersome. To simplify, we collapse them into a compact matrix form:

$$\begin{cases} \hat{\mathbf{\Gamma}}^{A}\hat{\mathbf{v}}^{A} + \hat{\mathbf{R}}^{A}\hat{\mathbf{a}}_{d}^{A} + \hat{\mathbf{R}}^{A}\boldsymbol{\mathcal{G}}^{A}\hat{\mathbf{f}} = \hat{\mathbf{w}}^{A} \\ \hat{\mathbf{T}}^{A}\hat{\mathbf{v}}^{A} + (\hat{\mathbf{S}}^{A} - 1)\hat{\mathbf{a}}_{d}^{A} + (\hat{\mathbf{S}}^{A} - 1)\hat{\boldsymbol{\mathcal{G}}}^{A}\hat{\mathbf{f}} = \hat{\mathbf{f}}^{A} \\ (\hat{\mathbf{S}}^{S} - 1)\hat{\mathbf{a}}_{d}^{S} + (\hat{\mathbf{S}}^{S} - 1)\hat{\boldsymbol{\mathcal{G}}}^{S}\hat{\mathbf{f}} = \hat{\mathbf{f}}^{S}. \end{cases}$$
(11)

Here, matrices with superscripts A or S denote blocks corresponding to antennas or scatterers, respectively. We define these matrices explicitly as follows:

$$\hat{\mathbf{\Gamma}}^{A} = \operatorname{diag}\left(\mathbf{\Gamma}^{1}, \cdots, \mathbf{\Gamma}^{M}\right), \hat{\mathbf{T}}^{A} = \operatorname{diag}\left(\mathbf{T}^{1}, \cdots, \mathbf{T}^{M}\right), \\ \hat{\mathbf{R}}^{A} = \operatorname{diag}\left(\mathbf{R}^{1}, \cdots, \mathbf{R}^{M}\right), \hat{\mathbf{S}}^{A} = \operatorname{diag}\left(\mathbf{S}^{1}, \cdots, \mathbf{S}^{M}\right), \\ \hat{\mathbf{S}}^{S} = \operatorname{diag}\left(\mathbf{S}^{M+1}, \cdots, \mathbf{S}^{M+N}\right)$$
(12)

$$\hat{\mathbf{v}}^{A} = \begin{bmatrix} \mathbf{v}^{1} \\ \vdots \\ \mathbf{v}^{M} \end{bmatrix}, \hat{\mathbf{w}}^{A} = \begin{bmatrix} \mathbf{w}^{1} \\ \vdots \\ \mathbf{w}^{M} \end{bmatrix}, \hat{\mathbf{a}}_{d}^{A} = \begin{bmatrix} \mathbf{a}_{d}^{1} \\ \vdots \\ \mathbf{a}_{d}^{M} \end{bmatrix}, \\
\hat{\mathbf{a}}_{d}^{S} = \begin{bmatrix} \mathbf{a}_{d}^{M+1} \\ \vdots \\ \mathbf{a}_{d}^{M+N} \end{bmatrix}, \hat{\mathbf{f}}^{A} = \begin{bmatrix} \mathbf{f}^{1} \\ \vdots \\ \mathbf{f}^{M} \end{bmatrix}, \hat{\mathbf{f}}^{S} = \begin{bmatrix} \mathbf{f}^{M+1} \\ \vdots \\ \mathbf{f}^{M+N} \end{bmatrix}$$
(13)

and $\hat{\mathbf{f}} = \begin{bmatrix} \mathbf{f}^A \\ \hat{\mathbf{f}}^S \end{bmatrix}$. The definitions of the matrices $\hat{\boldsymbol{\mathcal{G}}}^A$ and $\hat{\boldsymbol{\mathcal{G}}}^S$ are slightly different—while the number of rows corresponds to the set A or S, the number of columns is always M+N. For instance, the pq-th matrix block (with $p \in A/S$ and $q \in A \cup S$) of $\hat{\boldsymbol{\mathcal{G}}}^{A/S}$ reads

$$\hat{\boldsymbol{\mathcal{G}}}_{pq}^{A/S} = (1 - \delta_{pq}) \, \boldsymbol{\mathcal{G}}_{pq} \tag{14}$$

where δ_{pq} is kronecker delta.

With the aforementioned notations, the last two equations in (11) can be combined into

$$\begin{bmatrix} \hat{\mathbf{T}}^A \hat{\mathbf{v}}^A \\ \mathbf{0} \end{bmatrix} + (\hat{\mathbf{S}} - \mathbf{1})\hat{\mathbf{a}}_d + (\hat{\mathbf{S}} - \mathbf{1})\hat{\mathbf{\mathcal{G}}}\hat{\mathbf{f}} = \hat{\mathbf{f}}$$
 (15)

which can then be solved for

$$\hat{\mathbf{f}} = \left\{ \mathbf{1} - \left(\hat{\mathbf{S}} - \mathbf{1} \right) \hat{\mathbf{\mathcal{G}}} \right\}^{-1} \left\{ \begin{bmatrix} \hat{\mathbf{T}}^A \hat{\mathbf{v}}^A \\ \mathbf{0} \end{bmatrix} + \left(\hat{\mathbf{S}} - \mathbf{1} \right) \hat{\mathbf{a}}_d \right\}$$
(16)

where

$$\hat{\mathbf{a}}_{d} = \begin{bmatrix} \hat{\mathbf{a}}_{d}^{A} \\ \hat{\mathbf{a}}_{d}^{S} \end{bmatrix}, \hat{\mathbf{\mathcal{G}}} = \begin{bmatrix} \hat{\mathbf{\mathcal{G}}}^{A} \\ \hat{\mathbf{\mathcal{G}}}^{S} \end{bmatrix}, \hat{\mathbf{S}} = \operatorname{diag}\left(\hat{\mathbf{S}}^{A}, \hat{\mathbf{S}}^{S}\right). \tag{17}$$

Further defining the matrix $\mathbf{M} = \mathbf{1} - \left(\hat{\mathbf{S}} - \mathbf{1}\right)\hat{\boldsymbol{\mathcal{G}}}$, bifurcating it as

$$\mathbf{M} = egin{bmatrix} \mathbf{M}_{AA} & \mathbf{M}_{AS} \\ \mathbf{M}_{SA} & \mathbf{M}_{SS} \end{bmatrix}$$

and letting

$$\tilde{\mathbf{M}} = \mathbf{M}_{AA} - \mathbf{M}_{AS} \mathbf{M}_{SS}^{-1} \mathbf{M}_{SA}$$

$$\mathbf{M}_{L} = \begin{bmatrix} \mathbf{1} & -\mathbf{M}_{SS}^{-1} \mathbf{M}_{SA} \end{bmatrix}^{t} \tilde{\mathbf{M}}^{-1}$$
(18)

we then have (cf. Appendix B)

$$\mathbf{M}^{-1} \begin{bmatrix} \hat{\mathbf{T}}^A \hat{\mathbf{v}}^A \\ \mathbf{0} \end{bmatrix} = \mathbf{M}_L \hat{\mathbf{T}}^A \mathbf{v}^A. \tag{19}$$

Therefore, (16) can be rewritten as

$$\mathbf{M}_{L}\hat{\mathbf{T}}^{A}\hat{\mathbf{v}}^{A} + \mathbf{M}^{-1}\left(\hat{\mathbf{S}} - \mathbf{1}\right)\hat{\mathbf{a}}_{d} = \hat{\mathbf{f}}.$$
 (20)

Substituting (20) into the first equation of (11) yields

$$\hat{\mathbf{w}}^{A} = \left(\hat{\mathbf{\Gamma}}^{A} + \hat{\mathbf{R}}^{A}\hat{\mathbf{\mathcal{G}}}^{A}\mathbf{M}_{L}\hat{\mathbf{T}}^{A}\right)\hat{\mathbf{v}}^{A} + \hat{\mathbf{R}}^{A}\hat{\mathbf{a}}_{d}^{A} + \hat{\mathbf{R}}^{A}\mathbf{M}^{-1}\left(\hat{\mathbf{S}} - \mathbf{1}\right)\hat{\mathbf{a}}_{d}$$
(21)

viz.,

$$\hat{\mathbf{w}}^{A} = \begin{pmatrix} \hat{\mathbf{\Gamma}}^{A} + \hat{\mathbf{R}}^{A} \hat{\mathbf{\mathcal{G}}}^{A} \mathbf{M}_{L} \hat{\mathbf{T}}^{A} \end{pmatrix} \hat{\mathbf{v}}^{A}
+ \left\{ \begin{bmatrix} \hat{\mathbf{R}}^{A} & \mathbf{0} \end{bmatrix} + \hat{\mathbf{R}}^{A} \mathbf{M}^{-1} \begin{pmatrix} \hat{\mathbf{S}} - \mathbf{1} \end{pmatrix} \right\} \hat{\mathbf{a}}_{d}.$$
(22)

If we introduce a representation similar to GS-matrix as

$$\begin{bmatrix} \mathbf{\Gamma}_G & \mathbf{R}_G \\ \mathbf{T}_G & \mathbf{S}_G - \mathbf{1} \end{bmatrix} \begin{bmatrix} \hat{\mathbf{v}}^A \\ \hat{\mathbf{a}}_d \end{bmatrix} = \begin{bmatrix} \hat{\mathbf{w}}^A \\ \hat{\mathbf{f}} \end{bmatrix}$$
 (23)

by comparing with (20) and (22), we can deduce:

$$\Gamma_{G} = \hat{\Gamma}^{A} + \hat{\mathbf{R}}^{A} \hat{\boldsymbol{\mathcal{G}}}^{A} \mathbf{M}_{L} \hat{\mathbf{T}}^{A}
\mathbf{R}_{G} = \begin{bmatrix} \hat{\mathbf{R}}^{A} & \mathbf{0} \end{bmatrix} + \hat{\mathbf{R}}^{A} \hat{\boldsymbol{\mathcal{G}}}^{A} \mathbf{M}^{-1} \begin{pmatrix} \hat{\mathbf{S}} - \mathbf{1} \end{pmatrix}
\mathbf{T}_{G} = \mathbf{M}_{L} \hat{\mathbf{T}}^{A}
\mathbf{S}_{G} - \mathbf{1} = \mathbf{M}^{-1} \begin{pmatrix} \hat{\mathbf{S}} - \mathbf{1} \end{pmatrix}.$$
(24)

For pure antenna systems, by removing the matrix blocks associated with scatterers and noting that $\hat{\mathcal{G}} = \hat{\mathcal{G}}^A$, $\mathbf{M}_L = \mathbf{M}^{-1}$, (24) simplifies to the results in [13]. Similarly, for pure scatterer systems, only the last equation in (24) remains, which can be used to address multiple scattering problems. This result is consistent with [7], but our fully matrix-based representation is considerably more concise compared to the series representation in [7].

An alternative representation of (24), while not computationally efficient, provides a clearer physical interpretation by separating the coupling effects from the original responses. Replacing $\hat{\mathbf{f}}$ in the left-hand side of (15) with (20) yields

$$\hat{\mathbf{f}} = \left\{ \begin{bmatrix} \hat{\mathbf{T}}^A \\ \mathbf{0} \end{bmatrix} + (\hat{\mathbf{S}} - \mathbf{1})\hat{\boldsymbol{\mathcal{G}}}\mathbf{M}_L\hat{\mathbf{T}}^A \right\} \hat{\mathbf{v}}^A
+ \left\{ (\hat{\mathbf{S}} - \mathbf{1}) + (\hat{\mathbf{S}} - \mathbf{1})\hat{\boldsymbol{\mathcal{G}}}\mathbf{M}^{-1} \left(\hat{\mathbf{S}} - \mathbf{1} \right) \right\} \hat{\mathbf{a}}_d.$$
(25)

Thus:

$$\mathbf{T}_{G} = \begin{bmatrix} \hat{\mathbf{T}}^{A} \\ \mathbf{0} \end{bmatrix} + (\hat{\mathbf{S}} - \mathbf{1})\hat{\mathbf{\mathcal{G}}}\mathbf{M}_{L}\hat{\mathbf{T}}^{A}$$

$$\mathbf{S}_{G} - \mathbf{1} = (\hat{\mathbf{S}} - \mathbf{1}) + (\hat{\mathbf{S}} - \mathbf{1})\hat{\mathbf{\mathcal{G}}}\mathbf{M}^{-1} \left(\hat{\mathbf{S}} - \mathbf{1}\right).$$
(26)

Together with the first two equations in (24), we derive

$$\begin{bmatrix}
\mathbf{\Gamma}_{G} & \mathbf{R}_{G} \\
\mathbf{T}_{G} & \mathbf{S}_{G} - \mathbf{1}
\end{bmatrix} = \begin{bmatrix}
\hat{\mathbf{\Gamma}}^{A} & \hat{\mathbf{R}}^{A} & \mathbf{0} \\
\hat{\mathbf{T}}^{A} & \hat{\mathbf{S}}^{A} - \mathbf{1} & \mathbf{0} \\
\mathbf{0} & \mathbf{0} & \hat{\mathbf{S}}^{S} - \mathbf{1}
\end{bmatrix} + \begin{bmatrix}
\hat{\mathbf{R}} \\
\hat{\mathbf{G}}
\end{bmatrix} \begin{bmatrix}
\hat{\mathbf{G}}^{A} \\
\hat{\mathbf{G}}
\end{bmatrix} \begin{bmatrix}
\mathbf{M}_{L} & \mathbf{M}^{-1}
\end{bmatrix} \begin{bmatrix}
\hat{\mathbf{T}} \\
\hat{\mathbf{S}} - \mathbf{1}
\end{bmatrix}$$
(27)

where the first term represents the original response of each structure, while the second term describes the coupling effects among different structures. If we expand \mathbf{M}^{-1} in (27) using the Neumann series as

$$\mathbf{M}^{-1} = \mathbf{1} + (\hat{\mathbf{S}} - \mathbf{1})\hat{\mathbf{G}} + \{(\hat{\mathbf{S}} - 1)\hat{\mathbf{G}}\}^2 + \cdots$$
 (28)

and note that M_L is the leftmost column of M^{-1} in its matrix-partition representation, one can easily identify the coupling effects at different orders.

Note that (23) is not directly equivalent to the GS-matrix of the system since $\hat{\mathbf{a}}_d$ and $\hat{\mathbf{f}}$ are given in the local coordinate systems of the individual components rather than the global coordinate system. Since the system's total scattered wave is composed of the contributions from each individual component, translating their expansion vectors into the global coordinate system and summing them gives:

$$\mathbf{f} = \sum_{p} \mathcal{R}_{p} \mathbf{f}^{p} \tag{29}$$

in matrix form, (29) can also be written as

$$\mathbf{f} = \hat{\mathcal{R}}\hat{\mathbf{f}} \tag{30}$$

with $\hat{\mathcal{R}} = [\mathcal{R}_1, \mathcal{R}_2, \cdots, \mathcal{R}_{M+N}]$. Here, $\mathcal{R}_p = \mathcal{R}(k\mathbf{r}_p)$ is another translation matrix (see Appendix A).

On the other hand, the direct incident wave \mathbf{a}_d^p is a translation of the entire system's incident wave \mathbf{a} into the p-th local coordinate system, *i.e.*, $\mathbf{a}_d^p = \mathcal{R}_p^t \mathbf{a}$. Analogous to (30), we have

$$\hat{\mathbf{a}}_d = \hat{\boldsymbol{\mathcal{R}}}^t \mathbf{a}. \tag{31}$$

Substituting (30) and (31) into (23) and comparing with (3), we can deduce the GS-matrix for the entire system (strictly speaking, the variant of GS-matrix):

$$\begin{bmatrix} \mathbf{\Gamma} & \mathbf{R} \\ \mathbf{T} & \mathbf{S} - \mathbf{1} \end{bmatrix} = \begin{bmatrix} \mathbf{1} & \\ & \hat{\mathcal{R}} \end{bmatrix} \begin{bmatrix} \mathbf{\Gamma}_G & \mathbf{R}_G \\ \mathbf{T}_G & \mathbf{S}_G - \mathbf{1} \end{bmatrix} \begin{bmatrix} \mathbf{1} & \\ & \hat{\mathcal{R}}^t \end{bmatrix}. \quad (32)$$

IV. NUMERICAL EXAMPLES

A. Case 1: pure scattering system

Figure 3 illustrates a system comprising four spherical scatterers. The radii of sphere S_1 to S_4 are 24 mm, 12 mm, 18 mm and 10 mm, positioned at the origin, x-axis, y-axis and z-axis, respectively. Spheres S_3 and S_4 are made of perfect electric conductor (PEC), while S_1 and S_2 are composed

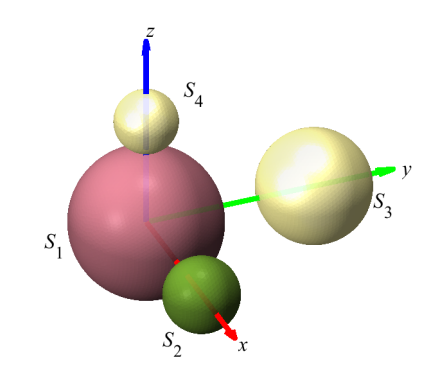


Fig. 3. Pure scattering system consisting of four spheres.

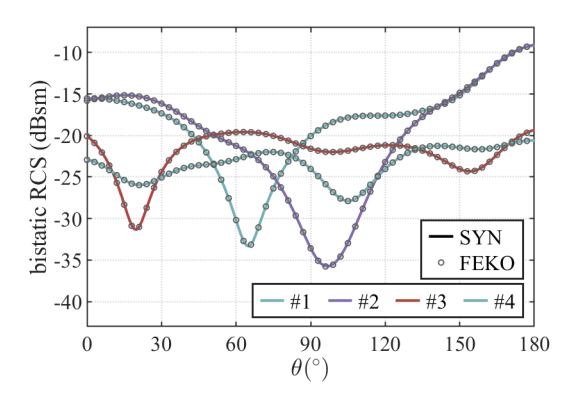


Fig. 4. Bistatic RCS of the system in Fig. 3 under plane wave illumination. The curves are presented for the xoz plane. #1: plane wave incident from -z direction with x polarization, #2: -z direction with y polarization, #3: -x direction with z polarization, #4: -y direction with z polarization.

of dielectric materials with relative permittivities of 8 and 4.4-8.8j, respectively. The scattering behavior like such a system has been extensively studied in the past [4]–[7], [16], primarily because the scattering matrix for a spherical object can be obtained analytically. Here, we reproduce the results using equation (32) to verify the applicability of our unified formulation in antenna-free scenarios.

We investigate the bistatic radar cross section (RCS) of this system at 6 GHz for different plane-wave excitations. The results are obtained by left-multiplying the synthesized S-matrix by the expansion vector of the incident plane waves, and then applying equation (21) from [15]. As shown in Fig. 4, the synthesized results (labeled as "SYN") are in excellent agreement with the full-wave simulation results from FEKO, which validates our formulation for this case.

B. Case 2: pure antenna system

Next, we examine a pure antenna system consisting of two pyramidal horn antennas, as illustrated in Fig. 5. The two antennas have identical dimensions but are separated by a distance d, with an axial angle between them (*i.e.*, the angle between axes x_1 and x_2) given by $\alpha_0 = \pi - \varphi_0$.

To obtain the GS-matrix of the entire system, following the procedures in Sec. III, we first determine the independent GS-matrix of each pyramidal horn. Since the antennas are identical, their GS-matrices are the same in their respective local coordinate systems. However, the second coordinate

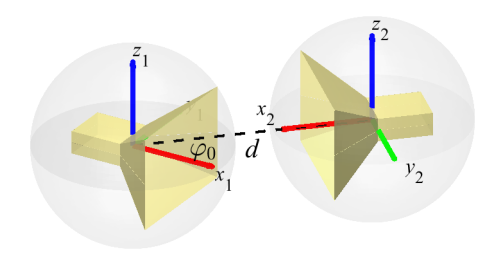


Fig. 5. An antenna system of two pyramidal horn antennas. Each horn can be geometrically modeled as a combination of a cuboid and a flare. In this example, the dimensions of the flare are: front rectangle 20 cm \times 14.3 cm, back rectangle 7.1 cm \times 3.5 cm, with a length of 8 cm. The cuboid section is also 8 cm long, with a cross-sectional area of 7.1 cm \times 3.5 cm.

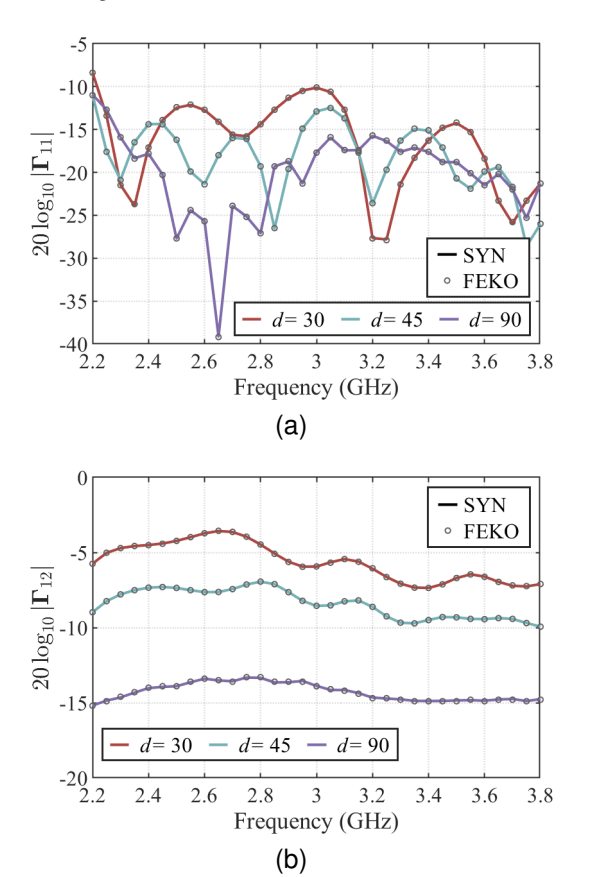


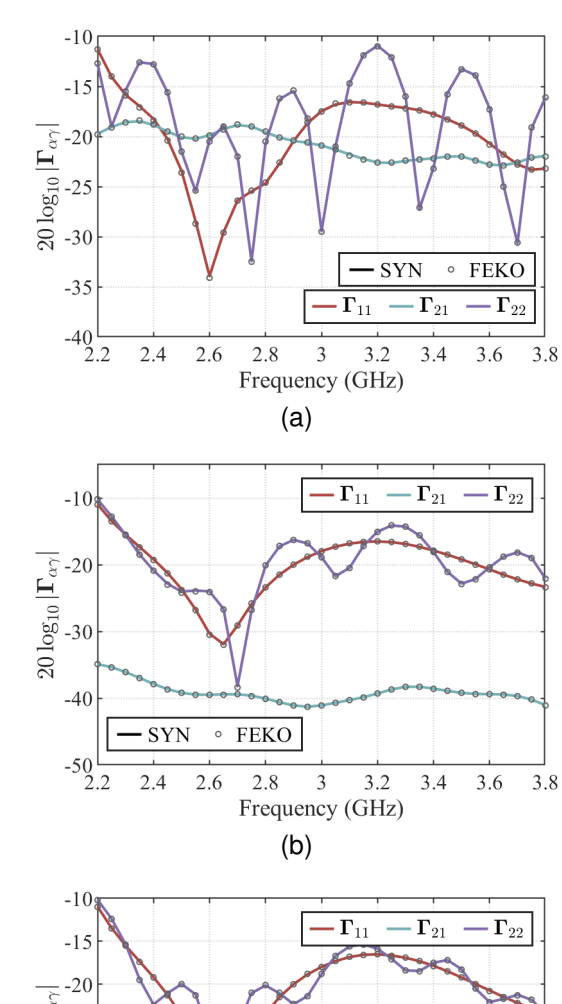
Fig. 6. S-parameters of two pyramidal horn antennas placed head-to-head for varying distances d (in cm). (a) Reflection coefficients (Γ_{11}), (b) Transmission coefficients (Γ_{12}).

system is rotated by an angle α_0 about the z-axis compared to the first, which is inconsistent with the conditions specified in Sec. III. Therefore, we need to rotate the second coordinate system about the z_2 -axis by $-\alpha_0$ to align its axes directions with those of coordinate system (x_1,y_1,z_1) . This process requires using the rotation properties of VSWFs.

The relation between the vector of the rotated coordinate system (primed symbol) and the original coordinate system is given by

$$\mathbf{f}' = \mathcal{D}\mathbf{f}, \mathbf{a}' = \mathcal{D}\mathbf{a} \text{ or } \mathbf{f} = \mathcal{D}^t \mathbf{f}', \mathbf{a} = \mathcal{D}^t \mathbf{a}'$$
 (33)

where \mathcal{D} is the rotation matrix, and $\mathcal{D}^t = \mathcal{D}^{-1}$. When real-valued spherical harmonics are used to generate VSWFs, \mathcal{D} is a real matrix typically defined in terms of the three Euler



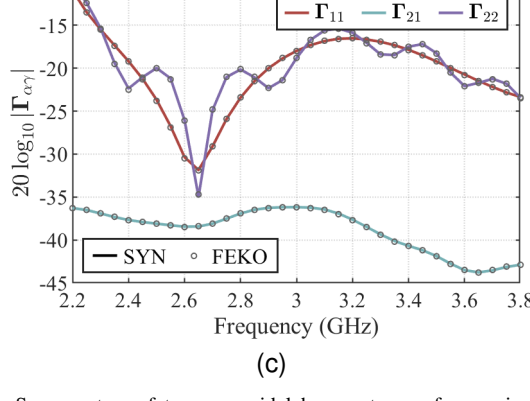


Fig. 7. S-parameters of two pyramidal horn antennas for varying φ_0 . (a) $\varphi_0=45^\circ$, (b) $\varphi_0=90^\circ$, (c) $\varphi_0=135^\circ$. Here, the distance d is fixed at $\frac{45}{3}$ cm

rotation angles, α, β, γ , *i.e.*, $\mathcal{D} = \mathcal{D}(\alpha, \beta, \gamma)$, as defined in [8], [17]. In this specific example, $\mathcal{D} = \mathcal{D}(-\alpha_0, 0, 0)$. Consequently, the GS-matrix after coordinate system rotation can be expressed as:

$$\tilde{\mathbf{S}}' = \begin{bmatrix} \mathbf{1} & \\ & \mathcal{D} \end{bmatrix} \tilde{\mathbf{S}} \begin{bmatrix} \mathbf{1} & \\ & \mathcal{D}^t \end{bmatrix}$$
 (34)

since

$$\begin{split} \begin{bmatrix} \mathbf{w}' \\ \mathbf{f}' \end{bmatrix} &= \begin{bmatrix} \mathbf{1} & \\ & \mathcal{D} \end{bmatrix} \begin{bmatrix} \mathbf{w} \\ \mathbf{f} \end{bmatrix} \\ &= \begin{bmatrix} \mathbf{1} & \\ & \mathcal{D} \end{bmatrix} \tilde{\mathbf{S}} \begin{bmatrix} \mathbf{v} \\ \mathbf{a} \end{bmatrix} = \begin{bmatrix} \mathbf{1} & \\ & \mathcal{D} \end{bmatrix} \tilde{\mathbf{S}} \begin{bmatrix} \mathbf{1} & \\ & \mathcal{D}^t \end{bmatrix} \begin{bmatrix} \mathbf{v}' \\ \mathbf{a}' \end{bmatrix}. \end{split}$$

(34) is computationally efficient compared to re-simulating the second pyramidal horn, as the cost of computing the rotation matrix is almost negligible. This greatly facilitates the analysis of varying antenna orientations.

Using (34) and following the procedure in Sec. III, we synthesized the GS-matrix for the entire antenna system. For the case where the two pyramidal horns are directly facing each other (i.e., $\varphi_0 = 0$, $\alpha_0 = \pi$), Fig. 6 shows the S-parameters for different distances d. We also show the simulation results from the FEKO software, which are in perfect agreement with the synthesized results. The variation in distance affects not only the received power between the two horns but also the port reflection coefficients.

Furthermore, Fig. 7 shows the S-parameters as the placement angle φ_0 of the second pyramidal horn varies, with the antenna distance fixed at 45 cm. The observed variation in the S-parameters is consistent with engineering intuition: as φ_0 increases, the received power in antenna 2 decreases because it is increasingly oriented away from the main lobe of antenna 1. Moreover, when antenna 2 is rotated from $\varphi_0 = 90^\circ$ to $\varphi_0 = 135^\circ$, there is little change in the reflection coefficient of antenna 1, since antenna 2 no longer blocks antenna 1. The FEKO results agree well with the results computed using our synthesis method, demonstrating that our theory is applicable to pure antenna systems.

Throughout the computational cases in this section, each pyramidal horn was discretized using 5766 RWG basis functions. The FEKO simulations required 189 seconds per frequency point, while the synthesis method took only 67 seconds, of which 63 seconds were used to obtain the GS-matrix for a single pyramidal horn. This demonstrates that the synthesis method significantly accelerates the solution process, making it more convenient to analyze the effects of varying antenna distances and orientations.

C. Case 3: scatterer-antenna hybrid system

Our final example aims to verify the correctness of the proposed formula in a general scatterer-antenna hybrid system. We revisit the two pyramidal horn antennas with the same dimensions as shown in Fig. 5, but now with the addition of a PEC sphere positioned in the middle, as depicted in Fig. 8. Due to scattering from the sphere, we observe a significant decrease in the transmission coefficient between the antennas compared to Fig. 6b. The synthesized S-parameters show good agreement with the FEKO simulation results.

Next, we feed antenna 2 and examine its gain pattern at 3.2 GHz, as shown in Fig. 9. Without the sphere scatterer, the gain pattern is still concentrated in the forward direction, indicating that the scattering (obscuring) effect of horn 1 is not significant. However, with the addition of the sphere scatterer, the beam is split into three distinct lobes. The gain patterns obtained from FEKO simulation are nearly identical to those computed using the synthesis method, further validating the correctness of our theory for general cases.

V. CONCLUSION

This paper presents a method to synthesize the GS-matrix of a hybrid system using the independent S-matrices and GS-

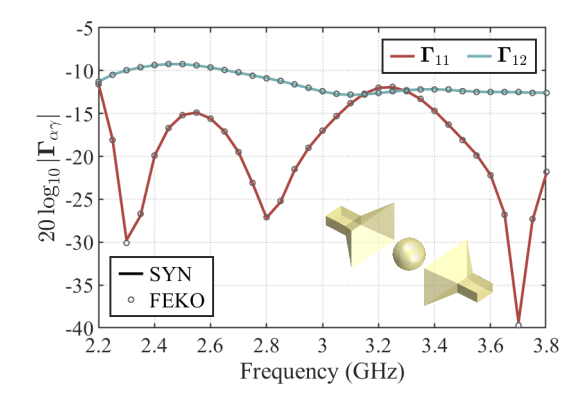


Fig. 8. S-parameters of the hybrid system with two pyramidal horn antennas separated by d=45 cm. The sphere radius is 5 cm.

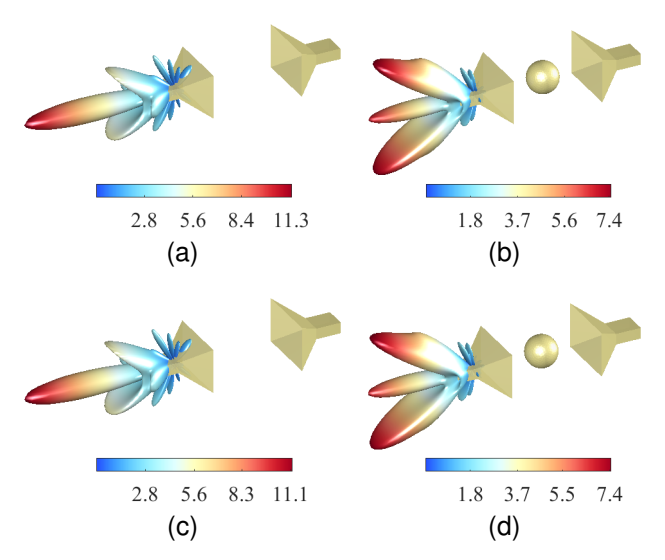


Fig. 9. Gain pattern when only antenna 2 is fed. (a) and (c) show the cases without the sphere scatterer, while (b) and (d) show the cases with the sphere scatterer added. The top panel presents results calculated using the synthesized GS-matrix, while the bottom panel shows results obtained using the FEKO software.

matrices of its constituent components. The derived formulation is unified and is also applicable to both pure antenna and pure scattering systems without limitations on the number of antennas or scatterers. Numerical examples demonstrate the correctness and broad applicability of the proposed formulation. These results indicate that the unified GS-matrix formulation can serve as a domain decomposition method for efficiently analyzing multi-structured systems, enhancing computational efficiency while ensuring accuracy.

When rotation of the structure is involved, the GS-matrix approach, utilizing the rotation theory of VSWFs, can quickly provide the results without requiring re-modeling or repeated numerical simulations. This is particularly effective for applications where the effect of antenna orientation and polarization needs to be analyzed.

APPENDIX A TRANSLATION MATRIX

[7], [18], [19] provides representations for the translation matrix of VSWFs, suitable for translating along any directions.

However, these approaches can be computationally intensive, except when the translation occurs along the z-axis, for which [20] offers a simplified version of their formula. To efficiently solve for the translation matrix of VSWFs, one effective approach is to rotate the coordinate system to align the translation direction with the z-axis, solve the problem in that configuration, and then apply an inverse rotation [10], [13]. Thus, the general translation matrix $\mathcal{R}(k\mathbf{d})$ can be expressed as

$$\mathcal{R}(k\mathbf{d}) = \mathcal{D}^{t}\operatorname{Re}\left\{\mathcal{Y}^{z}(kd)\right\}\mathcal{D}$$
(35)

where $\mathbf{\mathcal{Y}}^z(kd)$ is the z-axis translation matrix defined in the Appendix of [20], and for convenience, we repeat its representations here:

$$\mathcal{Y}^{z}_{1\sigma ml,1\sigma ml'} = c_{m\sigma} \cdot C_{l,l',m}(kd)
\mathcal{Y}^{z}_{1\sigma ml,1\sigma'ml'} = 0, \sigma \neq \sigma'
\mathcal{Y}^{z}_{1\sigma ml,2\sigma'ml'} = (-1)^{\sigma+m} D_{l,l',m}(kd), \sigma \neq \sigma'
\mathcal{Y}^{z}_{1\sigma ml,2\sigma ml'} = 0
\mathcal{Y}^{z}_{2\sigma ml,\tau\sigma'ml'} = \mathcal{Y}^{z}_{1\sigma ml,\bar{\tau}\sigma'ml'}, \tau = 1, 2.$$
(36)

Here, $\tau \sigma ml$ is a composite index of VSWFs [19], representing its type (TE and TM), parity (cos or sin), order and degree, respectively. The coefficient $c_{m\sigma} = (-1)^m + \delta_{m0}(-1)^{\sigma}$, and $C_{l,l',m}$, $D_{l,l',m}$ are given by:

$$C_{l,l',m}(kd) = \frac{\varepsilon_m}{4} \times \sum_{\lambda=|l-l'|}^{l+l'} (-1)^{(l'-l+\lambda)/2} (2\lambda+1)$$

$$\times \sqrt{\frac{(2l+1)(2l'+1)}{l(l+1)l'(l'+1)}}$$

$$\times \binom{l}{0} \binom{l'}{0} \binom{l}{m} \binom{l'}{m} \binom{\lambda}{m} \binom{l}{m} \binom{l'}{m} \binom{\lambda}{m} \binom{l'}{m} \binom{\lambda}{m} \binom{l'}{m} \binom{\lambda}{m} \binom{l'}{m} \binom{\lambda}{m} \binom{l'}{m} \binom{\lambda}{m} \binom{l'}{m} \binom{\lambda}{m} \binom{k}{m} \binom{k}{m$$

and

$$D_{l,l',m}(kd) = -m \times \sum_{\lambda=|l-l'|}^{l+l'} (-1)^{(l'-l+\lambda)/2} (2\lambda + 1)$$

$$\times \sqrt{\frac{(2l+1)(2l'+1)}{l(l+1)l'(l'+1)}}$$

$$\times \binom{l \quad l' \quad \lambda}{0 \quad 0 \quad 0} \binom{l \quad l' \quad \lambda}{m \quad -m \quad 0}$$

$$\times kd \times h_{\lambda}^{(2)}(kd)$$
(38)

where $\varepsilon_m=2-\delta_{m0},\,h_\lambda^{(2)}$ is the spherical Hankel function of the second type, and

$$\begin{pmatrix} \cdot & \cdot & \cdot \\ \cdot & \cdot & \cdot \end{pmatrix}$$

represents the Wigner 3-j symbol [21].

Another translation matrix G is defined as

$$\mathcal{G}(k\mathbf{d}) = \frac{1}{2}\mathcal{D}^{t}\mathcal{Y}^{z}(kd)\mathcal{D}.$$
 (39)

This matrix is used to translate the expansion coefficients of one structure's scattered wave into the incident waves on another structure, but it only holds when the minimum circumscribing spheres of the two structures do not overlap. When studying closely spaced structures, \mathcal{Y}^z in (39) cannot be obtained through the analytical formula in (36), and transformation between plane wave functions and VSWFs may be required [22], necessitating numerical integration. For simplicity, all examples in this paper satisfy the condition in (36).

APPENDIX B

THE INVERSE OF MATRIX IN BLOCK-PARTITION FORM For the matrix

$$\mathbf{M} = \mathbf{1} - \left(\hat{\mathbf{S}} - \mathbf{1}\right)\hat{\mathcal{G}} = egin{bmatrix} \mathbf{M}_{AA} & \mathbf{M}_{AS} \ \mathbf{M}_{SA} & \mathbf{M}_{SS} \end{bmatrix}$$

used in Sec. III, the inverse, M^{-1} , in block-partition form, is given by:

$$\begin{bmatrix} \tilde{\mathbf{M}}^{-1} & -\tilde{\mathbf{M}}^{-1}\mathbf{M}_{AS}\mathbf{M}_{SS}^{-1} \\ -\mathbf{M}_{SS}^{-1}\mathbf{M}_{SA}\tilde{\mathbf{M}}^{-1} & \mathbf{M}_{SS}^{-1} + \mathbf{M}_{SS}^{-1}\mathbf{M}_{SA}\tilde{\mathbf{M}}^{-1}\mathbf{M}_{AS}\mathbf{M}_{SS}^{-1} \end{bmatrix}$$
(40)

where $\tilde{\mathbf{M}} = \mathbf{M}_{AA} - \mathbf{M}_{AS} \mathbf{M}_{SS}^{-1} \mathbf{M}_{SA}$ is known as the Schur complement of \mathbf{M}_{SS} in \mathbf{M} . All inverse matrices involved in (40) are of smaller scale compared to \mathbf{M} , making it more efficient than directly computing \mathbf{M}^{-1} .

The left column of M^{-1} reads

$$\mathbf{M}_{L} = \begin{bmatrix} \mathbf{1} \\ -\mathbf{M}_{SS}^{-1} \mathbf{M}_{SA} \end{bmatrix} \tilde{\mathbf{M}}^{-1}$$
 (41)

leading to equation (19):

$$\mathbf{M}^{-1}egin{bmatrix} \hat{\mathbf{T}}^A\hat{\mathbf{v}}^A \ \mathbf{0} \end{bmatrix} = \mathbf{M}_L\hat{\mathbf{T}}^A\hat{\mathbf{v}}^A.$$

REFERENCES

- [1] R. Tsu, "The theory and application of the scattering matrix for electromagnetic waves," *The Ohio State University*, 1960.
- [2] B. Friedman and J. Russek, "Addition theorems for spherical waves," Q. Appl. Math., vol. 12, no. 1, pp. 13–23, 1954.
- [3] K. T. Kim, "The translation formula for vector multipole fields and the recurrence relations of the translation coefficients of scalar and vector multipole fields," *IEEE Trans. Antennas Propag.*, vol. 44, no. 11, pp. 1482–1487, Nov. 1996.
- [4] C. Liang and Y. T. Lo, "Scattering by two spheres," *Radio Science*, vol. 2, no. 12, pp. 1481-1495, 1967.
- [5] J. Bruning and Y. Lo, "Multiple scattering of EM waves by spheres part I-Multipole expansion and ray-optical solutions," *IEEE Trans. Antennas Propag.*, vol. 19, no. 3, pp. 378-390, 1971.
- [6] D. W. Mackowski and M. I. Mishchenko, "Calculation of the T matrix and the scattering matrix for ensembles of spheres," *JOSA A*, vol. 13, no. 11, pp. 2266-2278, 1996.
- [7] B. Peterson and S. Ström, "T matrix for electromagnetic scattering from an arbitrary number of scatterers and representations of E (3)," *Physical Review D*, vol. 8, no. 10, pp. 3661, 1973.
- [8] C. Shi, et al., "Synthesis Method for Obtaining Characteristic Modes of Multi-Structure Systems," arXiv preprint arXiv:2411.08905, 2024.
- [9] C. G. Montgomery, R. H. Dicke, and E. M. Purcell, eds., *Principles of Microwave Circuits*, no. 25, IET, 1987.
- [10] J. E. Hansen, Ed., Spherical Near-Field Antenna Measurements. London, U.K.: Peter Peregrinus Ltd., 1988.
- [11] W. K. Kahn and H. Kurss, "Minimum-scattering antennas," *IEEE Trans. Antennas Propag.*, vol. 13, no. 5, pp. 671-675, 1965.
- [12] W. Wasylkiwskyj and W. K. Kahn, "Theory of mutual coupling among minimum-scattering antennas," *IEEE Trans. Antennas Propag.*, vol. 18, no. 2, pp. 204-216, 1970.

- [13] J. Rubio, M. A. González, and J. Zapata, "Generalized-scattering-matrix analysis of a class of finite arrays of coupled antennas by using 3-D FEM and spherical mode expansion," *IEEE Trans. Antennas Propag.*, vol. 53, no. 3, pp. 1133-1144, 2005.
- [14] M. Alian and N. Noori, "A domain decomposition method for the analysis of mutual interactions between antenna and arbitrary scatterer using generalized scattering matrix and translation addition theorem of SWFs," *IEEE Trans. Antennas Propag.*, 2023.
- [15] C. Shi, et al., "Generalized Scattering Matrix of Antenna: Moment Solution, Compression Storage and Application," arXiv preprint arXiv:2411.08904, 2024.
- [16] D. W. Mackowski and M. I. Mishchenko, "A multiple sphere T-matrix Fortran code for use on parallel computer clusters," *J. Quant. Spectrosc. Radiative Transfer*, vol. 112, no. 13, pp. 2182-2192, 2011.
- [17] Z. Su and P. Coppens, "Rotation of real spherical harmonics," Acta Crystallogr. A, vol. 50, no. 5, pp. 636-643, 1994.
- [18] A. Boström, G. Kristensson, and S. Ström, "Transformation properties of plane, spherical and cylindrical scalar and vector wave functions," in Acoustic, Electromagnetic and Elastic Wave Scattering, Field Representations and Introduction to Scattering, Elsevier, 1991, pp. 165-210.
- [19] G. Kristensson, Scattering of Electromagnetic Waves by Obstacles, Edison, NJ, USA: SciTech Publishing, 2016.
- [20] C. Shi, J. Pan, et al., "Scattering-based characteristic mode theory for structures in arbitrary background: Computation, benchmarks, and applications," *IEEE Trans. Antennas Propag.*, 2024.
- [21] A. R. Edmonds, Angular Momentum in Quantum Mechanics, 2nd ed., Princeton, NJ, USA: Princeton Univ. Press, 1960.
- [22] J. Rubio and R. Gómez-Alcalá, "Mutual coupling of antennas with overlapping minimum spheres based on the transformation between spherical and plane vector waves," *IEEE Trans. Antennas Propag.*, vol. 69, no. 4, pp. 2103-2111, 2020.